sensors

MDPI

Communication

Inter-Mode Crosstalk Estimation between Cores for LP_{mn} Modes in Weakly Coupled Few-Mode Multicore Fiber with Perturbations

Shuangmeng Liu [1] and Lian Xiang [1,2,*]

[1] School of Electronic and Information Engineering, Soochow University, Suzhou 215006, China; lxiang@suda.edu.cn
[2] Faculty of Business Information, Shanghai Business School, Shanghai 201400, China
* Correspondence: xianglian119@163.com

Abstract: A novel inter-mode crosstalk (IMXT) model of LP_{mn} mode for weakly coupled few-mode multicore fiber is proposed based on the coupled mode theory (CMT) with bending and twisting perturbations. A universal expression of the mode coupling coefficient (MCC) between LP_{mn} modes is derived. By employing this MCC, the universal semi-analytical model (USAM) of inter-core crosstalk (ICXT) can be applied to calculate the IMXT. Simulation results show that our model is generally consistent with previous theories when stochastic perturbations are absent. Moreover, our model can work effectively when stochastic perturbations are present, where former theories are not able to work properly. It has been theoretically found that the MCC has an intimate relationship with core pitch. Our model, based on the CMT, can provide physical characteristics in detail, which has not been reported clearly by former theories. In addition, our model is applicable to phase-matching and non-phase-matching regions of both real homogeneous and heterogeneous few-mode multicore fibers (FM-MCFs) with a wider range of applications.

Keywords: inter-mode crosstalk; few-mode multicore fiber; mode coupling coefficient

Citation: Liu, S.; Xiang, L. Inter-Mode Crosstalk Estimation between Cores for LP_{mn} Modes in Weakly Coupled Few-Mode Multicore Fiber with Perturbations. *Sensors* **2024**, *24*, 5969. https://doi.org/10.3390/s24185969

Academic Editor: Zhongyi Guo

Received: 9 August 2024
Revised: 12 September 2024
Accepted: 12 September 2024
Published: 14 September 2024

1. Introduction

Multicore fibers (MCFs) based on spatial division multiplexing (SDM) technology can greatly alleviate the capacity limitations of single-mode fiber (SMF) [1–4]. Transmission media for SDM are mostly multicore fiber and few-mode fiber (FMF) [5]. Nowadays, few-mode multicore fibers (FM-MCFs) [6] significantly enhance transmission capacity as a hybrid method of MCF and FMF. In past studies, a data rate of 5.1 Tb/s per carrier has been reached using hole-assisted FM-MCF over a 1 km single fiber with seven few-mode cores [7,8]. However, inter-core crosstalk (ICXT) is one of the most important influencing factors in coupled MCF, which significantly degrades transmission performance [9–12]. Therefore, quite a few researchers have focused on analyzing the characteristics of ICXT evolution caused by variations in fiber structures and external factors [13–15].

In recent years, various theoretical and experimental studies have been reported in the literature to accurately characterize and model ICXT. In [16], a discrete changes model (DCM) for the longitudinal evolution of ICXT in homogeneous weakly coupled MCFs with bending and twisting perturbations was proposed based on the coupled mode theory (CMT). As a typical model for ICXT estimation, a DCM works well in the phase-matching region, but it is not applicable to the non-phase-matching region and cannot be used for heterogeneous MCFs. Although continuously enhanced DCMs have also been reported subsequently, they still cannot operate in the non-phase-matched region [13–17]. In [18], the coupling coefficient between cores has been derived analytically to evaluate ICXT with single mode. Based on the analytical coupling coefficient, a universal semi-analytical model (USAM) of ICXT for real coupled MCFs has been put forward, which can be utilized both in phase-matching and phase-mismatching regions [19]. So far, a highly mature theoretical

foundation has been developed in the study of ICXT estimation for multicore single-mode fibers. Typically, the CMT and the coupled power theory (CPT) are widely employed for investigating the estimation of ICXT [20,21].

Similarly, inter-mode crosstalk (IMXT) plays the same role in FM-MCF [22]. Research on IMXT for FM-MCF is still in its initial stages. In [23], the effect of inter-core polarization mode dispersion (PMD) on IMXT was studied, and a closed expression for the correlation length of the birefringence vector was given. In [24], IMXT was derived from stochastic differential equations (SDEs) based on the CPT, which considered both deterministic and stochastic inter-core coupling. That work found that when the deterministic coupling strength was sufficiently strong, it could suppress the influence of the PMD on IMXT for LP_{mn} modes. However, the IMXT method in [24] did not consider the impact of bending and twisting perturbations on crosstalk. In addition, the impact of random perturbations on crosstalk was not considered in [24], which re-characterizes IMXT in practical FM-MCF transmission [25,26].

In this paper, we derive a universal expression of the mode coupling coefficient (MCC) for LP_{mn} modes between cores based on the CMT and Maxwell equations to estimate the IMXT in FM-MCF. The theoretical derivation of the MCC allowed us to precisely define the relationship between the deterministic coupling effect and the stochastic coupling effect mentioned in [24], and to obtain accurate IMXT values, whereas previous models have used mode coupling coefficient (K_{mn}) approximation, which leads to large errors. In addition, we analyzed the optimal line segment length for IMXT estimation in theory. In the next simulation, we found that the value of IMXT is greatly affected by stochastic perturbations, which cannot be estimated by previous theories. Therefore, our theory can provide a quite reliable model for the IMXT simulation of weakly coupled FM-MCF with random perturbations. Additionally, our model is influenced by physical parameters like core pitch and optical wavelength, which has not been addressed in previous theories. Generally, this paper is structured as follows. In Section 2, we discuss the derivation of the MCC and IMXT in detail. In Section 3, firstly, we present numerical simulations conducted to verify our theory. Next, we investigate the influence of IMXT on stochastic perturbations and physical characteristics. In Section 4, we present our conclusion.

2. Analysis and Methods

In this section, firstly, the MCC for the modes is derived from Maxwell equations. Next, an expression for IMXT estimation is obtained by employing the CMT. In LP_{mn} mode, m means that the pattern satisfies a Bessel function of order m, and n means that there are n solutions of that order. Our model can be applied to estimate the IMXT not only for LP_{o1}, but also for higher order modes.

2.1. Mode Coupling Coefficient of LP_{mn} Mode

The definition of mode coupling coefficient for LP_{mn} modes between cores can be written as [27]:

$$k_{mn} = \frac{\omega\varepsilon_0 \iint \left(n_1^2 - n_2^2\right) E_m^* \cdot E_n^* dxdy}{\iint e_z \cdot (E_m^* \times H_m) + E_m \times H_m^*) dxdy} \tag{1}$$

where ω is the angular frequency, ε_0 is the free-space permittivity, and n_1 and n_2 represent indexes of core and cladding, respectively. e_z represents a unit vector for x-polarization. E_m and H_m are electric and magnetic fields in the core domain, respectively, and E_n is the electric field in the cladding domain. The symbol * indicates the conjugate transform. According to [27], the denominator of (1) is related to the optical power.

$$\iint e_Z \cdot (E_m^* \times H_m) + E_m \times H_m^*) dxdy = 4P \tag{2}$$

2.2. Electric Field of LP_{mn} Mode Based on Maxwell Equations

As the fiber is a cylindrical structure, in column polar coordinates the electric field of the LP mode can be written as [27]:

$$\boldsymbol{E} = \boldsymbol{e_r}\boldsymbol{E_r} + \boldsymbol{e_\varphi}\boldsymbol{E_\varphi} + \boldsymbol{e_z}\boldsymbol{E_z} \tag{3}$$

where $\boldsymbol{E_x}$ denotes the electric field component in the x-direction and $\boldsymbol{e_x}$ denotes the unit vector in the x-direction. The transverse electric field component $\boldsymbol{E_r}$ and $\boldsymbol{E_\varphi}$ is difficult to obtain, but the longitudinal component can be solved by the chi-squared Helmholtz equation in [27] as follows:

$$E_{z1} = AJ_m\left(\frac{U}{a}r\right)\cos(m\varphi), 0 \le r \le a \tag{4-1}$$

$$E_{Z2} = A\frac{J_m(U)}{K_m(W)}K_m\left(\frac{W}{a}r\right)\cos(m\varphi), r \ge a \tag{4-2}$$

$$E_{r1} = -j\frac{a^2}{U^2}\left[\frac{\beta UA}{a}J'_m\left(\frac{U}{a}r\right) + \frac{\omega_0 mB}{r}J_m\left(\frac{U}{a}r\right)\right]\cos(m\varphi), 0 \le r \le a \tag{5-1}$$

$$E_{r2} = j\frac{a^2}{W^2}\frac{J_n(U)}{K_n(W)}\left[\frac{\beta WA}{a}K'_m\left(\frac{W}{a}r\right) + \frac{\omega_0 mB}{r}K_m\left(\frac{W}{a}r\right)\right]\cos(m\varphi), r \ge a \tag{5-2}$$

$$E_{\varphi 1} = -j\frac{a^2}{U^2}\left[-\frac{\beta mA}{r}J_m\left(\frac{U}{a}r\right) - \frac{\omega_0 UB}{a}J'_m\left(\frac{U}{a}r\right)\right]\sin(m\varphi), 0 \le r \le a \tag{5-3}$$

$$E_{\varphi 2} = j\frac{a^2}{W^2}\frac{J_m(U)}{K_m(W)}\left[-\frac{\beta mA}{r}K_m\left(\frac{W}{a}r\right) - \frac{\omega_0 WB}{a}K'_m\left(\frac{W}{a}r\right)\right]\sin(m\varphi), r \ge a \tag{5-4}$$

where $J_m(x)$ means the m order Bessel function of the first kind and $K_m(x)$ means the m order modified Bessel function of the second kind. U and W are the normalized transverse phase and attenuation parameters, respectively. $U = a\sqrt{k^2n_1^2 - \beta^2}$ and $W = a\sqrt{\beta^2 - k^2n_2^2}$, where β is the propagation constant, a is the core radius, and $k = 2\pi/\lambda$ is the wave number, where λ is wavelength. $A = jUC/a\beta$, where C is a system constant mentioned in [27].$B = -jUC/\omega u_0 a$, where $J'_m(x)$ is the first derivative of $J_m(x)$ and $K'_m(x)$ is the first derivative of $K_m(x)$.

The electric field of LP_{mn} behaves as a superposition of three dimensions:

$$\begin{aligned} I_m = E_{z1}^* E_{z2} + E_{r1}^* E_{r2} + E_{\varphi 1}^* E_{\varphi 2} = {} & \frac{J_m(U)}{K_m(W)}J_m\left(\frac{U}{a}r\right)K_m\left(\frac{W}{a}r\right) \\ & \left(A^2 cos^2(m\varphi) - \frac{m^2a^4\omega^2\mu_0^2B^2}{U^2W^2r^2}cos^2(m\varphi) - \frac{m^2a^4\beta^2A^2}{U^2W^2r^2}sin^2(m\varphi)\right) \\ & - \frac{J_m(U)}{K_m(W)}J'_m\left(\frac{U}{a}r\right)K'_m\left(\frac{W}{a}r\right)\left(\frac{a^2\beta^2A^2}{UW}cos^2(m\varphi) + \frac{a^2\omega^2\mu_0^2B^2}{UW}sin^2(m\varphi)\right) \\ & - \frac{J_m(U)}{K_m(W)}J'_m\left(\frac{U}{a}r\right)K_m\left(\frac{W}{a}r\right)\frac{a^3\beta Am\omega\mu_0 B}{UW^2r} \\ & - \frac{J_m(U)}{K_m(W)}J_m\left(\frac{U}{a}r\right)K'_m\left(\frac{W}{a}r\right)\frac{a^3\beta Am\omega\mu_0 B}{U^2Wr} \end{aligned} \tag{6}$$

Here, we set the value of m to obtain the electric field superposition of the corresponding LP_{mn} mode. Next, bringing (6) to the numerator of (1), we obtain

$$S_m = \iint\left(n_1^2 - n_0^2\right)E_m^* \cdot E_n^* dxdy = \iint\left(n_1^2 - n_0^2\right)I_m r dx d\varphi \tag{7}$$

where (R,θ) is a coordinate system originating at the center of core two, which represents the domain of $r > a$, as shown in Figure 1. The core pitch is denoted by D. When $D >> r$ holds, radius R can be approximated as $R = \sqrt{D^2 + r^2 - 2Drcos(\theta)} \cong D - rcos(\theta)$.

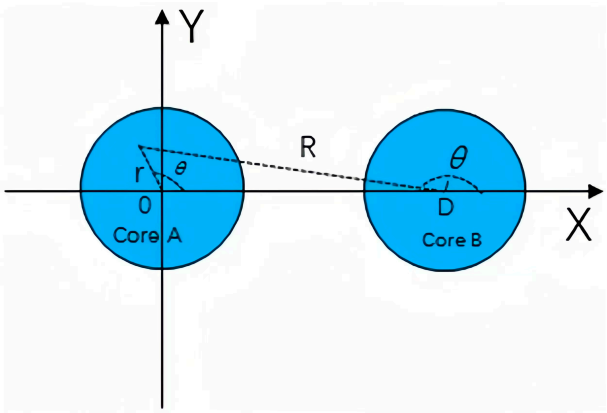

Figure 1. Schematic diagram of few-mode two-core fiber.

The final expression for the LP_{mn} mode coupling coefficients is obtained by bringing S_m into (1):

$$k_{mn} = \frac{\omega\varepsilon_0 S_m}{4P} \tag{8}$$

2.3. Inter-Mode Crosstalk Based on CMT

Based on the CMT, coupled-mode equations in coupled FM-MCFs can be expressed as [27]:

$$\frac{d\boldsymbol{E}}{dz} = j\boldsymbol{\beta}\boldsymbol{E} + j\boldsymbol{k}\boldsymbol{E} \tag{9}$$

where $\boldsymbol{E}$ and $\boldsymbol{\beta}$ are the electric field matrix and the propagation constant matrix, respectively. $\boldsymbol{k}$ is a mode coupling coefficient matrix made up with k_{mn}. A universal semi-analytical model (USM) has been proposed to solve the coupled mode equation in [19]. Therefore, we can generally evaluate the IMXT as:

$$\begin{aligned} IMXT = \sum_{i=1}^{N} IMXT_i &= \sum_{i=1}^{N} \frac{\frac{k_{mn,i}^2}{g_{mn,i}^2} sin^2(g_{mn,i}d)}{cos^2(g_{mn,i}d) + \frac{\Delta\beta_{mn,i}^2}{4g_{mn,i}^2} sin^2(g_{mn,i}d)} \\ &= \sum_{i=1}^{N} \left[\frac{k_{mn,i}}{g_{mn,i}} \sin(g_{mn,i}d)\right]^2 \end{aligned} \tag{10}$$

where $g_{mn,i} = \sqrt{k_{mn,i}^2 + \left(\frac{\Delta\beta_{mn,i}}{2}\right)}$ means modified mode coefficient, $k_{mn,i}$ is computed by (1) and $\Delta\beta_{mn,i}$ means the equivalent phase mismatching, which is defined in [19] as:

$$\Delta\beta_{mn,i}(d) = \beta_{m,i}(d) - \beta_{n,i}(d) \tag{11}$$

where $\beta_{m,i}(d)$ and $\beta_{n,i}(d)$ are equivalent propagation constants of core m and n, respectively, defined as:

$$\beta_i(d) \approx \beta_c\beta_p[R_b + rcos\theta(d)]/R_b \tag{12}$$

where $\beta_c = (2\pi/\lambda)n_{eff}^{(int)}$ is the unperturbed propagation constant of the fiber core, and $n_{eff}^{(int)}$ is the intrinsic effective refractive index of the fundamental mode. β_p represents the longitudinal fluctuations of propagation constants caused by inherent and external fluctuations. R_b is the bending radius. $\theta(d) = \gamma d + \varphi$, where γ and φ represent the twist rate of the core and the offset of the twist, respectively.

Based on the principle of USM, fully considering the characteristics of the stochastic perturbation, the fiber length is divided into N segments with each segment length d, as shown in Figure 2.

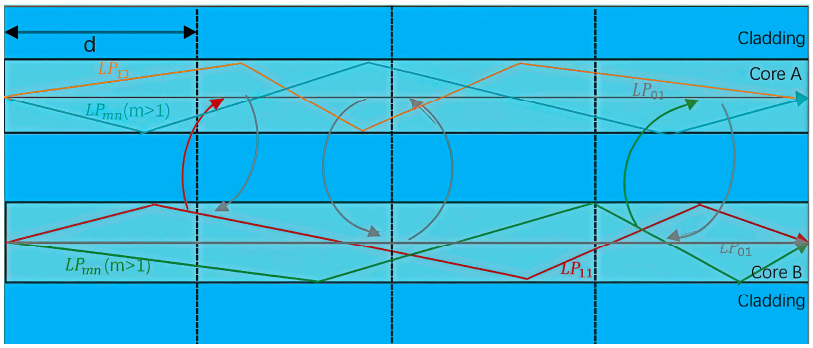

Figure 2. Schematic of mode coupling in few-mode two-core fiber.

3. Results and Discussion

In this section, the two-core fiber in [24] and four-core fiber are discussed in detail. Schematic diagrams of two-core fiber and four-core fiber are shown in Figures 1 and 3, respectively. Firstly, for two-core fiber, numerical simulations were carried out without stochastic perturbations to determine the optimal segment length and verify the accuracy of our model by comparison with the Monte Carlo Simulation in [23] and the analytical expression in [24]. In addition, the impact of physical characteristics, such as core pitch and optical wavelength, are discussed. Next, IMXT characteristics of the four-core fiber are studied. In a four-core fiber, it is assumed that one mode exists in each core, the LP_{01} mode exists in core 1, and LP_{1n} , LP_{2n}, and LP_{3n} modes exist in core 2, core 2, and core 3, respectively. In this paper, we refer to the evaluation method of [24] and use symmetric mode–asymmetric mode inter-mode coupling to approximate the inter-mode coupling as a generic LP mode. The fundamental mode of core 1 is used as the symmetric mode, and other low-order modes of core 2, core 3, and core 4 are used as asymmetric modes.

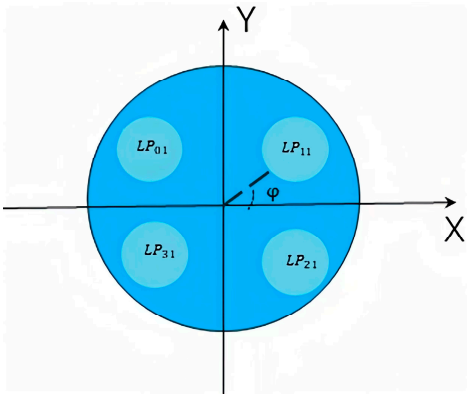

Figure 3. Schematic diagram of few-mode four-core fiber.

3.1. Fiber Parameter

For a few-mode two-core fiber, the core radius is 2.5 um, the cladding index is 1.45, and the wavelength is 1550 um, which are the same as those in [24]. For a few-mode four-core fiber, the IMXT between core 1 and core 2, core 1 and core 3, and core 1 and core 4 are discussed. To satisfy the normalization requirement, detailed parameters for the four-core fiber are shown in Table 1.

Table 1. Parameters of the four-core fiber.

Parameters	Symbol	Value
Core pitch	D	30 μm
Core radius	a	8 μm
Core index	n_1	1.4530
Cladding index	n_0	1.444
Wavelength	λ	1550 nm
Bending radius	R_b	400 mm
Twisting rate	γ	2π rad/m

3.2. IMXT Analysis of Two-Core Few-Mode Fiber

The two-core fiber was simulated first. The evaluation of IMXT is shown in Figure 4. Figure 4a shows the simulation results of IMXT as a function of the FM-MCF length for different segment lengths in the absence of stochastic perturbations. When segment length $d = 0.01$ m, the IMXT obtained by our theory matched well with the Monte Carlo Simulation in [23] and the analytical expression in [24], as shown by the purple dotted line, orange dotted dashed line, and black crosses in Figure 4a. When segment length $d = 0.02$ m and $d = 0.05$ m, the IMXT obtained from our theory was strikingly different from those of the former models. It is worth noting that the precision of the IMXT model is strongly dependent on segment length. It was shown that the segment length $d = 0.01$ m can be seen as an optimal segment length. So, the simulation results of our theory presented in the rest of our work were obtained with segment length $d = 0.01$ m.

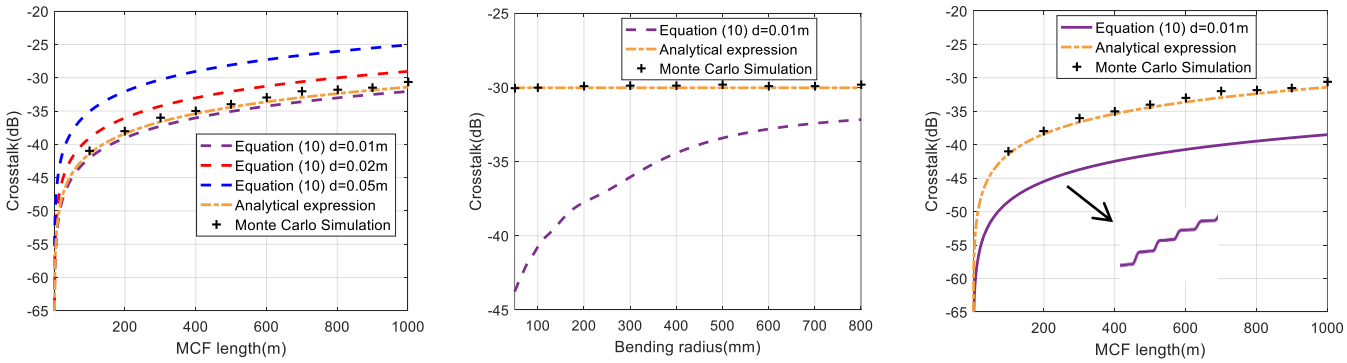

Figure 4. IMXT as a function of (**a**) FM−MCF length without stochastic perturbations, (**b**) bending radius, and (**c**) FM−MCF length with bending and twisting perturbation.

Furthermore, when the effects of bending and twisting perturbations in (12) are taken into account, it shows the IMXT as a function of bending radius for our model compared with former models when FM-MCF length is set to 1000 m, as shown in Figure 4b. The IMXT is significantly suppressed by bending perturbation, especially at a small bending radius. However, the former models cannot work normally with bending perturbation. A similar conclusion can be obtained with twisting and bending perturbations, as shown in Figure 4c, where $R_b = 0.2$ m,$\gamma = 2\pi$ rad/m. Moreover, the suppression on IMXT enhances with an FM-MCF length increase. Results in Figure 4b,c illustrate that both the Monte Carlo Model [23] and the analytical expression [24] are not sensitive to bending and twisting perturbations. However, in Figure 4c, we can see that our model reduces the IMXT value by 8 dB at 1000 m MCF length, which is because stochastic perturbations increase the effective refractive index difference between cores, which makes the IMXT computed by our theories lower than those of former theories. As the crosstalk increases significantly at the phase-matching point, some fluctuations in the purple curve estimated by our model can be found with changes over the distribution of the phase-matching point [17]. Therefore, our model can well reflect the effects of perturbations on IMXT.

In addition, former theories have not discussed the relationship between IMXT with physical characteristics. Figure 5 shows simulation results of IMXT as a function of core pitches, optical wavelengths, and twisting rates for our IMXT model and the analytical expression in [24]. Orange pentagrams represent the analytical expression based on CPT and purple dotted lines represent our IMXT model, which takes into account the impact of k_{mn}. These results indicate that the fiber parameters of our model have an effect on the estimation of IMXT under stochastic perturbations, which is similar to that of ICXT at MCF. However, the fiber parameters in the analytical expression do not have much effect on IMXT. This is because the analytical expression takes an approximation for k_{mn}, whereas our model for k_{mn} performs a detailed derivation.

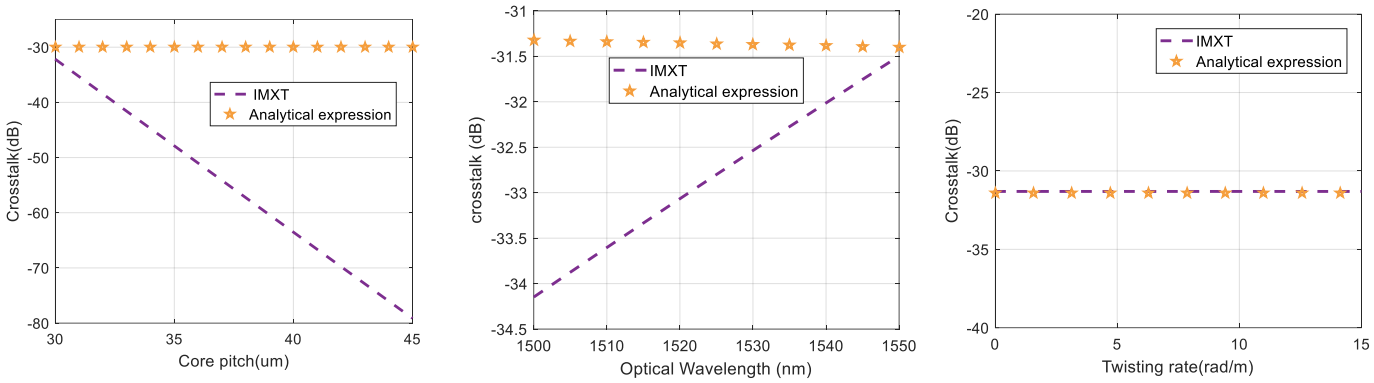

Figure 5. IMXT as a function of (**a**) core pitch, (**b**) optical wavelength, and (**c**) twisting rate for IMXT and analytical expression.

3.3. IMXT Analysis of Four-Core Few-Mode Fiber

Thereafter, the four-core FMF was simulated. See Appendix A for specific derivation. We took the LP_{01} mode as the longitudinal electric field distribution and other modes as the transverse electric field distribution to evaluate and analyze the crosstalk of the modes. Simulation results are shown in Figure 6. The dotted and dotted dashed lines in the figure represent the IMXT between the fundamental and other higher-order modes in our model and the analytical expression [24], respectively. In Figure 6a, it can be seen that crosstalk between the different modes obtained by our model and the analytical expression could be well matched under no stochastic perturbations. However, in the presence of stochastic perturbation, it can be clearly seen that crosstalk values between different modes obtained by our model became significantly smaller, whereas crosstalk obtained by the analytical expression had no obvious effect, as shown in Figure 6b. The trend of this simulation is consistent with the one obtained above using two-core fiber.

In the above study of the physical parameters of two-core fiber, we know that in the analytical expression the fiber parameters did not have a great influence on the IMXT. So, we directly studied our model subject to the core pitch and bending radius on the IMXT as shown in Figure 7. Figure 7a shows the IMXT as a function of the core pitch for our model, and it can be seen that IMXT continued to decrease as the inter-core distance increased. When the distance between the cores increased, MCCs decreased and the coupling effect between the modes decreased, resulting in a decrease in IMXT. Figure 7b,c show the IMXT as a function of the bending radius for our model in homogeneous and heterogeneous FM-MCFs. For values $\Delta n_{eff,mn}^{(int)} = 0.020\%$ and $\Delta n_{eff,mn}^{(int)} = 0.042\%$, the threshold bending radius $R_{PK1} = 96$ mm and $R_{PK2} = 43$ mm, respectively. Simulation results of the actual homogeneous few-mode four-core fiber are shown in Figure 7a. In the phase-matching region, IMXT is proportional to the bending radius. However, in the non-phase-matching region, IMXT is inversely proportional to the bending radius. The value of the crosstalk decreased with the bending radius and tended to a stable value gradually. Next, Figure 7b

illustrates the heterogeneous few-mode four-core fiber with a larger $\Delta n_{eff,mn}^{(int)}$. These results show that the variation trend is basically the same as that shown in Figure 7a. The trend of these results is similar to the theoretical analysis of ICXT in MCF [19,28,29].

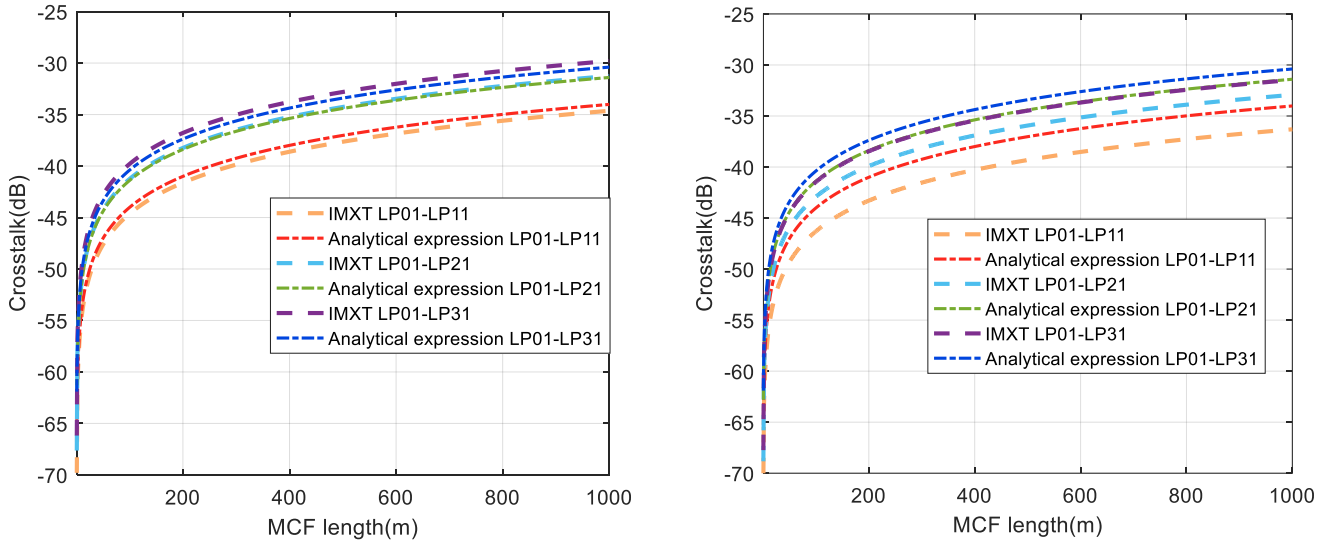

Figure 6. Estimation of crosstalk from the LP_{01} to the $LP_{11}(LP_{21}, LP_{31})$ as a function of FM−MCF length (**a**) without stochastic perturbations and (**b**) with stochastic perturbation.

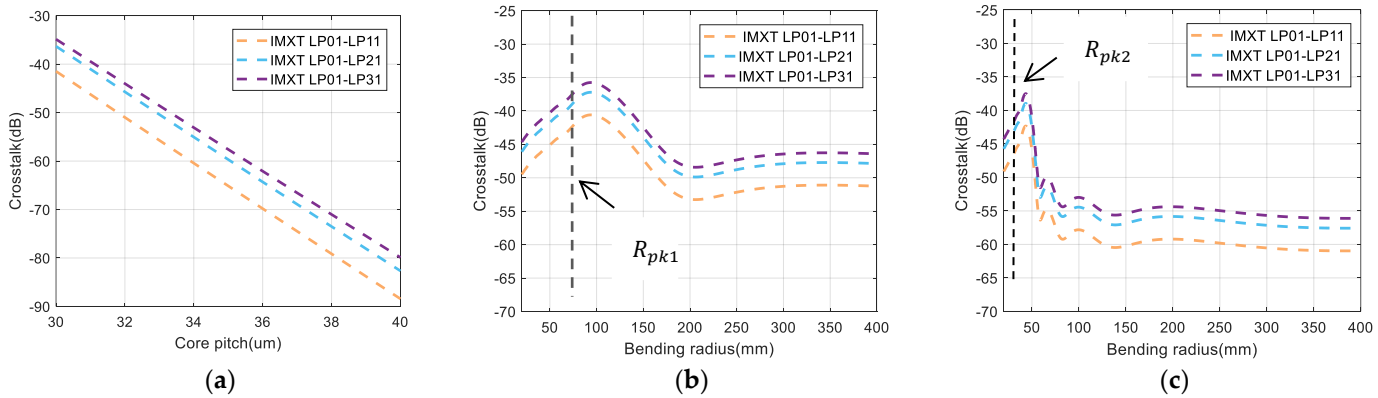

Figure 7. Estimation of crosstalk from LP_{01} to LP_{11} (LP_{21}, LP_{31}) as a function of (**a**) core pitch, (**b**) bending radius in homogeneous FM−MCF, and (**c**) bending radius in heterogeneous FM−MCF.

4. Conclusions

In this paper, we study the model of stochastic IMXT for LP_{mn} mode in weakly coupled FM-MCFs with random perturbations based on the CMT and Maxwell equations. In the absence of random perturbations, our model can well match the Monte Carlo Simulation [23] and the analytical expression [24] at optimal segment length $d = 0.01$ m, which verifies the accuracy of our model. In addition, our model calculates K_{mn} accurately, which can effectively minimize experimental error and make up for the shortcomings of previous studies that take into account only the approximate value of K_{mn}. In the presence of bending perturbations, our model more accurately estimates the effect of bending radius on the FM-MCF. The IMXT is about 8 dB lower than those of previous models, which is due to the fact that previous models directly ignored bending perturbations, which is not realistic. Next, we investigated the effects of physical properties, such as core pitch and optical wavelength, on IMXT. Results show that the IMXT of the fiber can be mitigated by rationally configuring the physical structure of the fiber, which has not

been discussed in previous models. Notably, study of the bending radius revealed that the model is applicable to both phase-matching and non-phase-matching regions of both homogeneous and heterogeneous FM-MCFs. Overall, we propose a systematic theory for IMXT estimation, which is more widely applicable and more accurately calculated in practical FM-MCF transmission with stochastic perturbations.

Author Contributions: Conceptualization, S.L.; methodology, S.L.; validation, S.L. and L.X.; writing—original draft preparation, S.L.; writing—review and editing, L.X. All authors have read and agreed to the published version of the manuscript.

Funding: This research was funded in part by the Science and Technology Project of Jiangsu Province, grant number BE2022055-3, and in part by the Suzhou Industry Foresight and Core Key Technology Project, grant number SYC2022138.

Data Availability Statement: Datasets presented in this article are not readily available because these data are part of an ongoing study.

Conflicts of Interest: The authors declare no conflicts of interest.

Appendix A

In a four-core FMF, the fundamental mode is used as the longitudinal electric field distribution such that $m = 0$ in (4):

$$E_{z1} = AJ_0\left(\frac{U}{a}r\right), 0 \le r \le a \tag{A1}$$

$$E_{Z2} = A\frac{J_0(U)}{K_0(W)}K_0\left(\frac{W}{a}r\right), r \ge a \tag{A2}$$

Other modes are used as transverse electric field distributions, which are obtained by making $m = 1$ in (5) when calculating the crosstalk between the LP_{01} and LP_{11} modes:

$$E_{r1} = -j\frac{a^2}{U^2}\left[\frac{\beta UA}{a}J_1'\left(\frac{U}{a}r\right) + \frac{\omega_0 B}{r}J_1\left(\frac{U}{a}r\right)\right]\cos(\varphi), 0 \le r \le a \tag{A3-1}$$

$$E_{r2} = j\frac{a^2}{W^2}\frac{J_1(U)}{K_1(W)}\left[\frac{\beta WA}{a}K_1'\left(\frac{W}{a}r\right) + \frac{\omega_0 B}{r}K_1\left(\frac{W}{a}r\right)\right]\cos(\varphi), r \ge a \tag{A3-2}$$

$$E_{\varphi 1} = -j\frac{a^2}{U^2}\left[-\frac{\beta A}{r}J_1\left(\frac{U}{a}r\right) - \frac{\omega_0 UB}{a}J_1'\left(\frac{U}{a}r\right)\right]\sin(\varphi), 0 \le r \le a \tag{A3-3}$$

$$E_{\varphi 2} = j\frac{a^2}{w^2}\frac{J_1(U)}{K_1(W)}\left[-\frac{\beta A}{r}K_1\left(\frac{W}{a}r\right) - \frac{\omega_0 WB}{a}K_1'\left(\frac{W}{a}r\right)\right]\sin(\varphi), r \ge a \tag{A3-4}$$

The electric field is then superimposed:

$$\begin{array}{c} I_m = E_{z1}^* E_{z2} + E_{r1}^* E_{r2} + E_{\varphi 1}^* E_{\varphi 2} = A^2\frac{J_0(U)}{K_0(W)}J_0\left(\frac{U}{a}r\right)K_0\left(\frac{W}{a}r\right) \\ -\frac{J_1(U)}{K_1(W)}J_1'\left(\frac{U}{a}r\right)K_1'\left(\frac{W}{a}r\right)\left(\frac{a^2\beta^2A^2}{UW}cos^2(\varphi) + \frac{a^2\omega^2\mu_0^2B^2}{UW}sin^2(\varphi)\right) \\ -\frac{J_1(U)}{K_1(W)}J_1'\left(\frac{U}{a}r\right)K_1\left(\frac{W}{a}r\right)\frac{a^3\beta A\omega\mu_0 B}{UW^2r} \\ -\frac{J_1(U)}{K_1(W)}J_1\left(\frac{U}{a}r\right)K_1'\left(\frac{W}{a}r\right)\frac{a^3\beta A\omega\mu_0 B}{U^2Wr} \end{array} \tag{A4}$$

Substituting I_m into (7) to continue the theoretical derivation, we obtain the crosstalk between the modes of $LP_{01}\_LP_{11}$. Following this derivation, the crosstalk between the modes of $LP_{01}\_LP_{21}$ and $LP_{01}\_LP_{31}$ can be obtained.

References

1. Saitoh, K.; Matsuo, S. Multicore Fiber Technology. *J. Light. Technol.* **2016**, *34*, 55–66. [CrossRef]
2. Richardson, D.J.; Fini, J.M.; Nelson, L.E. Space-Division Multiplexing in Optical Fibres. *Nat. Photonics* **2013**, *7*, 354–362. [CrossRef]
3. Dablu, K.; Rakesh, R. Appropriate Method of Core Selection and Crosstalk Optimization in Single-Mode Homogeneous Multicore Fiber. *Opt. Electron. Lett.* **2020**, *16*, 126–130. [CrossRef]
4. Rademacher, G.; Luis, R.S.; Puttnam, B.J.; Ryf, R.; van Eriksson, T.A.; Fontaine, N.K.; Chen, H.; Essiambre, R.-J.; Awaji, Y.; Wada, N. High Capacity Transmission in a Coupled-Core Three-Core Multi-Core Fiber. *J. Light. Technol.* **2021**, *39*, 757–762. [CrossRef]
5. Sillard, P.; Molin, D.; Bigot-Astruc, M.; Amezcua-Correa, A.; de Jongh, K.; Achten, F. 50 Mm Multimode Fibers for Mode Division Multiplexing. *J. Light. Technol.* **2016**, *34*, 1672–1677. [CrossRef]
6. Takenaga, K.; Sasaki, Y.; Guan, N.; Matsuo, S.; Kasahara, M.; Saitoh, K.; Koshiba, M. Large Effective-Area Few-Mode Multicore Fiber. *IEEE. Photonics Technol. Lett.* **2012**, *24*, 1941–1944. [CrossRef]
7. van Uden, R.G.H.; Correa, R.A.; Lopez, E.; Huijskens, F.; Xia, C.; Li, G.; Schülzgen, A.; de Waardt, H.; Koonen, A.M.J.; Okonkwo, C. Ultra-High-Density Spatial Division Multiplexing with a Few-Mode Multicore Fibre. *Nat. Photonics* **2014**, *8*, 865–870. [CrossRef]
8. Shao, P.; Wang, L.; Wang, Y.; Li, S.; Li, Z.; Wang, X.; Ma, L.; Meng, X.; Guo, Y.; Li, J.; et al. Preparation and Transmission Characteristics of Seven-Core Few-Mode Fiber with Low Loss and Low Inter-Core Crosstalk. *Opt. Express* **2022**, *30*, 27746. [CrossRef]
9. Fini, J.M.; Zhu, B.; Taunay, T.F.; Yan, M.F. Statistics of Crosstalk in Bent Multicore Fibers. *Opt. Express* **2010**, *18*, 15122. [CrossRef]
10. Puttnam, B.J.; Luís, R.S.; Agrell, E.; Rademacher, G.; Shen, J.; Klaus, W.; Saridis, G.M.; Awaji, Y.; Wada, N. High Capacity Transmission Systems Using Homogeneous Multi-Core Fibers. *J. Light. Technol.* **2017**, *35*, 1157–1167. [CrossRef]
11. Amaya, N.; Yan, S.; Channegowda, M.; Rofoee, B.R.; Shu, Y.; Rashidi, M.; Ou, Y.; Hugues-Salas, E.; Zervas, G.; Nejabati, R.; et al. Software Defined Networking (SDN) over Space Division Multiplexing (SDM) Optical Networks: Features, Benefits and Experimental Demonstration. *Opt. Express* **2014**, *22*, 3638. [CrossRef] [PubMed]
12. Sano, A.; Takara, H.; Kobayashi, T.; Miyamoto, Y. Crosstalk-Managed High Capacity Long Haul Multicore Fiber Transmission with Propagation-Direction Interleaving. *J. Light. Technol.* **2014**, *32*, 2771–2779. [CrossRef]
13. Soeiro, R.O.; Alves, T.M.; Cartaxo, A.V. Impact of Longitudinal Variation of the Coupling Coefficient due to Bending and Twisting on Inter-Core Crosstalk in Weakly-Coupled MCFs. *J. Light. Technol.* **2018**, *36*, 3898–3911. [CrossRef]
14. Soeiro, R.O.J.; Alves, T.M.F.; Cartaxo, A.V.T. Inter-Core Crosstalk in Weakly Coupled MCFs with Arbitrary Core Layout and the Effect of Bending and Twisting on the Coupling Coefficient. *Opt. Express* **2019**, *27*, 74. [CrossRef] [PubMed]
15. Soeiro, R.O.J.; Alves, T.M.F.; Cartaxo, A.V.T. Dual Polarization Discrete Changes Model of Inter-Core Crosstalk in Multi-Core Fibers. *IEEE Photonics Technol. Lett.* **2017**, *29*, 1395–1398. [CrossRef]
16. Hayashi, T.; Taru, T.; Shimakawa, O.; Sasaki, T.; Sasaoka, E. Design and Fabrication of Ultra-Low Crosstalk and Low-Loss Multi-Core Fiber. *Opt. Express* **2011**, *19*, 16576. [CrossRef]
17. Cartaxo, A.V.T.; Alves, T.M.F. Discrete Changes Model of Inter-Core Crosstalk of Real Homogeneous Multi-Core Fibers. *J. Light. Technol.* **2017**, *35*, 2398–2408. [CrossRef]
18. Ye, F.; Tu, J.; Saitoh, K.; Morioka, T. Simple Analytical Expression for Crosstalk Estimation in Homogeneous Trench-Assisted Multi-Core Fibers. *Opt. Express* **2014**, *22*, 23007. [CrossRef]
19. Wang, W.; Xiang, L.; Shao, W.; Shen, G. Stochastic Crosstalk Analyses for Real Weakly Coupled Multicore Fibers Using a Universal Semi-Analytical Model. *J. Light. Technol.* **2021**, *39*, 4503–4510. [CrossRef]
20. Koshiba, M.; Saitoh, K.; Takenaga, K.; Matsuo, S. Multi-Core Fiber Design and Analysis: Coupled-Mode Theory and Coupled-Power Theory. *Opt. Express* **2011**, *19*, B102. [CrossRef]
21. Li, M.-J.; Li, S.; Modavis, R.A. Coupled Mode Analysis of Crosstalk in Multicore Fiber with Random Perturbations. In Proceedings of the Optical Fiber Communication Conference, Los Angeles, CA, USA, 22–26 March 2015.
22. Zhou, J.; Pu, H. Generalized Analytical Study on the Random Crosstalk in Multicore/Multimode Fibers. *J. Light. Technol.* **2022**, *40*, 1112–1120. [CrossRef]
23. Antonelli, C.; Riccardi, G.; Hayashi, T.; Mecozzi, A. Role of Polarization-Mode Coupling in the Crosstalk between Cores of Weakly-Coupled Multi-Core Fibers. *Opt. Express* **2020**, *28*, 12847. [CrossRef] [PubMed]
24. Zhou, J.; Pu, H. Analytical Expressions for the Crosstalk of Super-Modes in the Tightly Bounded Multicore Fibers. *Opt. Express* **2022**, *30*, 4833–4844. [CrossRef] [PubMed]
25. Hayashi, T.; Sasaki, T.; Sasaoka, E.; Saitoh, K.; Koshiba, M. Physical Interpretation of Intercore Crosstalk in Multicore Fiber: Effects of Macrobend, Structure Fluctuation, and Microbend. *Opt. Express* **2013**, *21*, 5401–5412. [CrossRef] [PubMed]
26. Fini, J.M.; Zhu, B.; Taunay, T.F.; Yan, M.F.; Abedin, K.S. Crosstalk in Multicore Fibers with Randomness: Gradual Drift vs Short-Length Variations. *Opt. Express* **2012**, *20*, 949–959. [CrossRef]
27. Okamoto, K. *Fundamentals of Optical Waveguides*; Elsevier: Amsterdam, The Netherlands, 2010.

28. Hayashi, T.; Nagashima, T.; Shimakawa, O.; Sasaki, T.; Sasaoka, E. Crosstalk Variation of Multi-Core Fibre due to Fibre Bend. In Proceedings of the 2010 36th European Conference and Exhibition on Optical Communication—(ECOC 2010), Torino, Italy, 19–23 September 2010.
29. Fujisawa, T.; Amma, Y.; Sasaki, Y.; Matsuo, S.; Aikawa, K.; Saitoh, K.; Koshiba, M. Crosstalk Analysis of Heterogeneous Multicore Fibers Using Coupled-Mode Theory. *IEEE. Photonics Technol. Lett.* **2017**, *9*, 1–8. [CrossRef]